Available online at www.sciencedirect.com
SCIENCE DIRECT
Developmental Biology 287 (2005) 289 – 300
DEVELOPMENTAL BIOLOGY
www.elsevier.com/locate/ydbio

Xenopus Xpat protein is a major component of germ plasm and may function in its organisation and positioning

Rachel J. Machado [a,1,2], Wendy Moore [a,1], Richard Hames [a], Evelyn Houliston [b], Patrick Chang [b], Mary Lou King [c], Hugh R. Woodland [a,*]

[a] *Department of Biological Sciences, University of Warwick, Coventry CV47 AL, UK*
[b] *Unité de Biologie du Développement, UMR 7009 CNRS/Université Paris VI, Observatoire Océanologique, 06230 Villefranche sur Mer, France*
[c] *Department of Cell Biology and Anatomy, University of Miami School of Medicine, FL 33136, USA*

Received for publication 24 June 2005, revised 23 August 2005, accepted 26 August 2005
Available online 7 October 2005

Abstract

In many animals, including *Drosophila*, *C. elegans*, zebrafish and *Xenopus*, the germ line is specified by maternal determinants localised in a distinct cytoplasmic structure called the germ plasm. This is consists of dense granules, mitochondria, and specific localised RNAs. We have characterised the expression and properties of the protein encoded by *Xpat*, an RNA localised to the germ plasm of *Xenopus*. Immunofluorescence and immunoblotting showed that this novel protein is itself a major constituent of germ plasm throughout oogenesis and early development, although it is also present in other regions of oocytes and embryos, including their nuclei. We found that an Xpat-GFP fusion protein can localise correctly in cultured oocytes, in early oocytes to the 'mitochondrial cloud', from which germ plasm originates, and in later oocytes to the vegetal cortex. The localisation process was microtubule-dependent, while cortical anchoring required microfilaments. Xpat-GFP expressed in late stage oocytes assembled into circular fields of multi-particulate structures resembling endogenous fields of germ plasm islands. Furthermore these structures could be induced to form at ectopic sites by manipulation of culture conditions. Ectopic Xpat-GFP islands were able to recruit mitochondria, a major germ plasm component. These data suggest that Xpat protein has an important role in *Xenopus* germ plasm formation, positioning and maintenance.

Keywords: *Xenopus*; Oocyte; Germ plasm; Germ line; Xpat; Microtubules; Mitochondrial cloud

Introduction

In most animals, the germ line is founded by a small group of primordial germ cells (PGCs) set aside during early development. PGC fate is specified either by inductive signalling (e.g. in mammals and urodele amphibians) or by the inheritance of germ plasm, distinctive granular egg cytoplasm containing germ line determinants located at one pole of the zygote. The germ plasm-based mechanism is widespread through the animal kingdom (Extavour and Akam, 2003) and much is known of its biology because it occurs in several model species (*C. elegans*, *Drosophila*, zebrafish and *Xenopus*), in which it has been shown to contain specific determinants of germ line specification (Houston and King, 2000b; Santos and Lehmann, 2004; Williamson and Lehmann, 1996; Wylie, 1999). Germ plasm consists of granular structures rich in mitochondria and specific localised mRNAs, predominantly encoding RNA-binding proteins. Little is known about how it forms, except in *Drosophila*, where Oskar, which is localised to germ ('polar') granules both as RNA and protein, has been shown to be essential for germ plasm formation. The amount of Oscar determines the number of PGCs that will develop and its location determines where they form (Ephrussi and Lehmann, 1992; Smith et al., 1992). Oskar is unique to Dipteran insects and it is not known whether distinct proteins with equivalent functions exist in other germ plasm-containing species.

* Corresponding author. Fax: +44 2476 523701.
E-mail address: H.R.Woodland@warwick.ac.uk (H.R. Woodland).
[1] These authors contributed equally to this work.
[2] Present address: School of Biosciences, University of Birmingham, Edgbaston, Birmingham, B15 2TT, UK.

0012-1606/$ - see front matter © 2005 Elsevier Inc. All rights reserved.
doi:10.1016/j.ydbio.2005.08.044

Amongst vertebrates, germ plasm has been best studied in anuran amphibians, notably *Xenopus*. Anuran germ plasm derives from a macroscopic structure called the mitochondrial cloud, which juxtaposes the nucleus in previtellogenic oocytes (Dumont stages I–II). The mitochondrial cloud is packed with mitochondria, endoplasmic reticulum and dense germinal granules, set in a fibrillar matrix (al-Mukhtar and Webb, 1971; Chang et al., 2004; Czolowska, 1972; Heasman et al., 1984; Kloc et al., 1996, 2004; Smith and Williams, 1975; Zhou and King, 1996a). It develops from one of several perinuclear 'pre-clouds', distinguishable in the very early oocytes of immature frogs (Kloc et al., 1996). At the onset of vitellogenesis (stages II–III), it merges into the oocyte cortex at the future vegetal pole and disperses to give rise to germ plasm islands, rich in germinal granules and mitochondria, which come to occupy a large circular sub-cortical field by the end of oogenesis (stage VI) (Houston and King, 2000b; Kloc et al., 2002; Savage and Danilchik, 1993; Smith and Williams, 1975; Volodina et al., 2003). During oocyte maturation and early development, this field condenses progressively around the vegetal pole by a process involving periodic surface contraction waves towards the vegetal pole, dependent on the kinesin-family motor Xklp1 (Quaas and Wylie, 2002; Savage and Danilchik, 1993). The concentration of germ plasm results in it being confined to the cortex of about five cells in the vegetal germ layer of the blastula stage embryo. During the gastrula stage, the germ plasm moves from the cell cortex to form a perinuclear structure resembling the 'nuage' of early stages of gametogenesis. The germ plasm-containing cells undergo several more divisions, so that by the swimming tadpole stage, there are about 20–50 PGCs (Ikenishi et al., 1996; Kamimura et al., 1980; Whitington and Dixon, 1975).

The most available information on molecular processes involved in the formation of *Xenopus* germ plasm concerns the mechanism of incorporation into germ plasm of specific RNAs such as *Xcat2* and *Xdazl* (King et al., 2005; Zhou and King, 1996b). Accumulation of these RNAs in the mitochondrial cloud during stage I occurs by an entrapment process and does not require organised microtubule or microfilament networks (Chang et al., 2004; Kloc et al., 1996), although exogenous Xcat2 RNA has been observed to co-localise with microtubules (Choo et al., 2005). Dense endoplasmic reticulum (ER) in the MC provides a direct or indirect support for RNA attachment (Chang et al., 2004). During stage II, the germ plasm RNAs and germinal granules adopt a position at the vegetal tip of the MC termed the "METRO" region, from which they merge into the cortex and subsequently disperse with the germ plasm islands as the oocyte grows (Wilk et al., 2005). The process by which germ plasm RNAs localise to the vegetal oocyte cortex is termed the early or 'METRO' pathway, to distinguish it from the microtubule-dependent 'late' pathway (Kloc and Etkin, 1995). The late pathway operates during vitellogenic stages of oogenesis to bring mRNAs such as Vg1 and VegT, both involved in somatic fate determination, to a region of the vegetal cortex surrounding the germ plasm field (Houston and King, 2000b; King et al., 1999, 2005; Kloc et al., 2001; Yisraeli and Melton, 1988). RNA localisation by both early and late pathways involves the assembly of complexes with multiple proteins, requiring clustered sequence motifs in the RNAs (Betley et al., 2002; Bubunenko et al., 2002; Kloc et al., 2000; Kress et al., 2004; Kwon et al., 2002; Lewis et al., 2004). Some of these *cis*- and *trans*-acting factors are used in both pathways while others appear to be specific to either early or late pathway RNAs (Chang et al., 2004; Choo et al., 2005; Claussen et al., 2004).

While a number of RNAs have been identified as being specifically localised in the mitochondrial cloud and later in germ plasm islands or embryonic germ plasm [these include *Deadsouth*, *Xdazl*, *Hermes*, *Germes*, *Dead end* and *Xpat* (Berekelya et al., 2003; Houston and King, 2000a; MacArthur et al., 2000; Weidinger et al., 2003; Zearfoss et al., 2004)], none of the corresponding proteins have yet been shown to function in germ plasm formation, positioning or maintenance. *Xcat2* and *Xdazl* are implicated in germ cell development: *Xcat2* codes for a homologue of the *Drosophila* germ line/posterior determinant Nanos, and *Xdazl* is essential for correct PGC migration. Neither is translated before early embryonic stages, and so are unlikely to be involved in constructing and localising germ plasm (Houston and King, 2000a; MacArthur et al., 1999; Mosquera et al., 1993). Hermes protein is enriched in germ plasm, but disappears during oocyte maturation, and its function appears to be related to cell division in the early vegetal pole (Zearfoss et al., 2004). Other constituents of the mitochondrial cloud are proteins involved in RNA splicing, a Vasa-family member (Bilinski et al., 2004) and an Activin receptor localised in the germ plasm ER (Fukui et al., 2003). However, the presence of these proteins in mature germ plasm has not been reported. Lastly, at various stages, germ plasm contains a number of cytoskeletal proteins, including spectrin, γ-tubulin, vimentin and cytokeratin (Gard et al., 1997; Kloc and Etkin, 1998; Kloc et al., 1998; Torpey et al., 1992).

Xpat is a novel protein with no conserved domains (Hudson and Woodland, 1998) and we show here that, like its mRNA, it is an integral component of the germ plasm. Exogenous Xpat protein is capable of localising to the vegetal pole by a microtubule-dependent mechanism. It can assemble into structures which visually resemble germ plasm islands and, like germ plasm, incorporate mitochondria. Intriguingly, like Oskar in *Drosophila*, it is unique to its taxon.

Materials and methods

Oocyte and embryo culture

Stages I–II oocytes were isolated following collagenase treatment of ovaries (Chang et al., 2004). They were injected with 30 pg mRNA for Xpat-GFP or 23 pg of the fluorescent antisense Xpat, and cultured as previously described (Chang et al., 2004), with the exception of addition to the medium of 5% vitellogenin-containing *Xenopus* serum. Stage VI oocytes in intact follicles were dissected manually in modified Barths' medium and incubated in 50% Leibovitz L-15 medium (Gibco BRL) containing 10% vitellogenin serum or 5 mg/ml vitellogenin (Kloc and Etkin, 1999), with the addition of: 1 mM glutamine, 1 μg/ml insulin, 50 units/ml nystatin, 100 μg/ml gentamycin, 100 units/ml penicillin-streptomycin, 15 mM HEPES, pH 7.8 (Hudson and Woodland, 1998; Yisraeli and Melton, 1988). Typically, they were injected through the follicle with 1 ng mRNA in 18 nl water. Embryos were obtained

and injected by standard methods (Clements et al., 1999). GFP fluorescence was observed at low magnification with a Leica stereo fluorescence microscope or with a conventional Nikon fluorescence microscope using standard 10–40× objectives, or with a Leica SP2 confocal microscope using 40× or 63× oil and water immersion objectives. Particle movement was analysed using ImageJ software with the Manual Tracking PlugIn. Oocytes were matured by addition of 125 μg/ml progesterone, under the above culture conditions, and the oocytes were observed in the stereo microscope.

Cytoskeletal inhibitors (Sigma) were added to the media [2 μM cytochalasin D, 5 μg/ml paclitaxel (taxol), 10 μM demecolcemine (colcemid), 1 μg/ml nocodazole] after oocytes were injected with Xpat-GFP mRNA, and replaced daily. Mitochondria were stained with tetramethylrhodamine ethyl ester (TMRE, Molecular Probes) at 5 μg/ml for 4 min. Endoplasmic reticulum was labelled by microinjection of $DiIC_{16}(3)$ (Molecular Probes) in oil (Chang et al., 2004).

Immunological techniques

Sheep polyclonal antibodies were raised (Diagnostics, Scotland) against recombinant N-terminal 6× His-tagged Xpat cloned in pET-14b, expressed in *E. coli* strain BLR(DE3)pLysS (Novagen). The expressed protein was purified with His˙Bind resin under denaturing conditions (Novagen). Sheep serum was characterised by ELISA and Western blotting against recombinant Xpat protein by standard techniques. Xpat immune serum was affinity-purified using recombinant protein bound to nitrocellulose membrane under denaturing conditions and eluted with 0.1 M glycine–HCl (pH 2.7).

For immunofluorescence microscopy, oocytes and embryos were fixed and processed as described previously (Chang et al., 2004). Rabbit Anti-VDAC serum (Beckhelling et al., 2003) was a generous gift from Dr. M. Colombini and used at 1:200 dilution. The following commercial antibodies were used in this study: monoclonal anti-alpha and anti-gamma-tubulins, monoclonal anti-dynein intermediate chain, clone 70.1 (Sigma or Immunologicals Direct;), Alexa Fluor 594 donkey anti-sheep, Alexa Fluor 488 goat anti-mouse (Molecular Probes), rhodamine donkey anti-rabbit, Cy5 goat anti-rat, rhodamine donkey anti-sheep and FITC donkey anti-mouse (Jackson Immunoresearch), goat anti-mouse TRITC (Sigma). DNA was stained with 1 μg/ml DAPI (Sigma).

For Western blotting, oocytes and embryos were homogenised in low and high salt buffers (0.125 or 0.5 M KCl, 10 mM $MgCl_2$, 10 mM Tris–HCl pH 7.4, 0.2 mM $CaCl_2$), including protease inhibitor tablets (Roche). After centrifugation (20,200 × *g*, 10 min., 4°C), the supernatant from low salt extraction was TCA precipitated to give soluble Xpat and the pellet from high salt yielded the insoluble fraction. Pellets were homogenised in SDS loading buffer plus 2 M urea, resolved by 12% SDS-PAGE, transferred to Hybond nitrocellulose membranes (Amersham) and probed with a 1:300 dilution of affinity-purified anti-Xpat antibody. Secondary detection was with a 1:10,000 dilution of HRP-conjugated donkey anti-sheep antibody (Serotec), followed by ECL (Amersham).

Gene constructs and mRNA preparation

N-terminal 6× His-tagged Xpat (pET-14b-Xpat) corresponding to Xpat residues 1–170, was generated by PCR amplification of pBS-Xpat24 to introduce *Nde*1 and *Bam*H1 sites (with a stop codon) at nucleotide positions 1 and 510 respectively of the ORF. The excised fragment was sub-cloned in pET-14b (Novagen), creating an in-frame fusion.

For protein expression in eukaryotic cells, pEGFP-C1-Xpat (GFP-Xpat) was generated by PCR amplification of pBS-Xpat to introduce *Bgl*II and *Bam*HI sites. The Xpat ORF was excised with these enzymes and sub-cloned into the mammalian expression vector pEGFP-C1 (Clontech). Xpat-GFP for microinjection was made by inserting the PCR amplified ORF of GFP (primers: 5′ gccgagatctATGAGTAAAGGAGAAGAAC 3′; 5′ gccggaattcTTATTTGTATAGTTCATCCAT 3′) between the *Bgl*II and *Eco*R1 sites of pSPJC2L (Cook et al., 1993) to give pSPJC2L-cGFP. The ORF of Xpat without the STOP codon was amplified by PCR (primers: 5′ gccgagatctATGGCTTTGAAGGCAGAAG 3′; 5′ gccgagatctCAGGCCAACATCCCACCAAG 3′) and inserted into the *Bgl*II site of pSPJC2L-cGFP to yield pSPJC2. Xpat-GFP was transcribed from this *Not*I-linearised plasmid with SP6 RNA polymerase and the mMessage Machine kit (Ambion). Antisense fluorescent Xpat was transcribed from *Not*I-linearised pBluescript plasmid with T7 RNA polymerase using a standard Promega protocol with the following modifications: NTPs (Sigma) final concentrations were 1 mM, except UTP (0.8 mM) and Alexa 488 5-UTP (0.2 mM) (Molecular Probes). The transcript was purified using Probequant G-50 micro columns (Amersham Pharmacia).

Results

Expression and localisation of Xpat protein

In previous studies, we showed that *Xpat* mRNA is continuously present from at least pre-vitellogenic stage I of oogenesis to the tadpole stage (stage 41), at which time migrating PGCs enter the dorsal mesentery prior to their reaching the developing gonads (Hudson and Woodland, 1998). To determine when the protein product of this RNA was expressed, we raised a sheep antiserum against recombinant His-tagged Xpat protein. Western blot analysis with affinity-purified antibody revealed a band that co-migrated with overexpressed Xpat used as a control in these experiments (Fig. 1). Xpat was present as both a soluble and insoluble protein at all stages examined from stage I of oogenesis to stage 40 tadpole, consistent with its particulate nature (see below).

We studied the distribution of Xpat protein in oocytes and early embryos by whole mount immunofluorescence and confocal microscopy. Specificity of staining was confirmed by pre-absorbing the antibody with antigen to abolish staining (not shown). In the smallest oocytes in the adult ovary (stage I), the strongest staining was of small particles (less than 1 μm diameter) highly concentrated in the mitochondrial cloud, the site of germ plasm assembly (Fig. 2A). There was also staining in smaller, similar aggregates around the nucleus and in scattered particles throughout the cytoplasm and cortex. At earlier stages in immature frogs these “pre-clouds”, all contain localised germ plasm mRNA. While pre-clouds persist through stage I, one has now formed the mature cloud and only this contains germline mRNAs (Kloc et al., 1998). At stage II, when the mitochondrial cloud contacts the oocyte cortex at the future vegetal pole, Xpat is still concentrated throughout the cloud (Figs. 2B, C), whereas the *Xcat2* and *Xpat* mRNAs are in the part near the cortex (Wilk et al., 2005). By the end of oogenesis (stage VI), the circular field of germ plasm islands at the vegetal cortex, detected using a specific mitochondrial marker (Beckhelling et al., 2003), also stained strongly with the anti-Xpat antibody (Fig. 2D).

After fertilisation, the germ plasm islands move away from the vegetal cortex and during the early cleavage cycles they progressively condense into larger masses, still concentrated at the vegetal pole (see Introduction). Xpat was concentrated in germ plasm islands following fertilisation, during their progressive accumulation around the vegetal pole (Figs. 2E, F). The antibody also stained the perinuclear germ plasm in the PGCs of tailbud embryos (Figs. 2G–H), identified by their characteristic morphology, as shown by Kamimura et al. (1980) (Fig. 2I). At this stage, it no longer appears particulate in the PGCs. These results show that Xpat protein is a constituent of the germ plasm throughout oogenesis and early development.

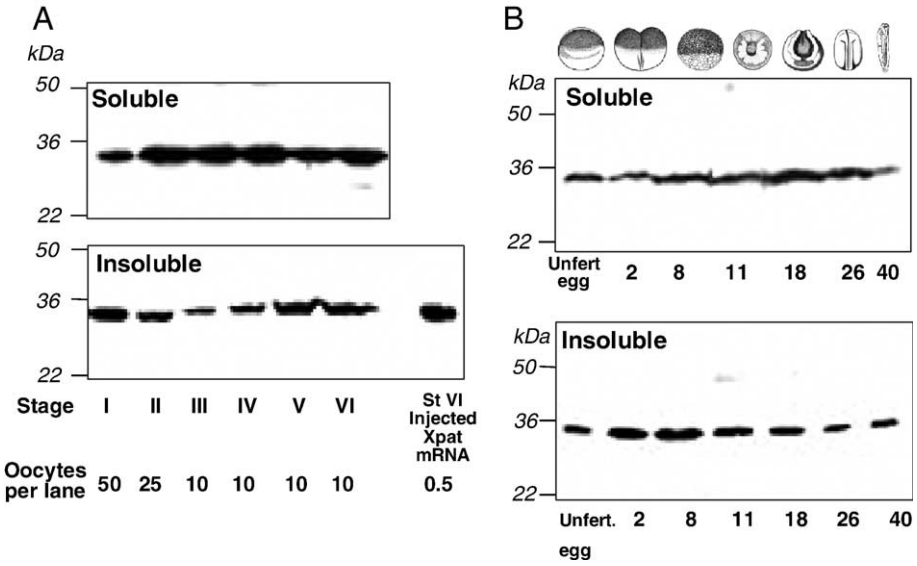

Fig. 1. Xpat protein is present throughout oogenesis and early development. Oocytes (A), eggs and embryos (B) were extracted either in 0.125 M KCl medium and the supernatant analysed by SDS gel electrophoresis and Western blotting, or in 0.5 M KCl and the pellet analysed. In the former extraction, the bulky yolk proteins are insoluble and in the latter they are soluble. A small sample from oocytes injected with 1 ng Xpat mRNA was run in parallel to confirm co-migration with the endogenous band detected (A).

Unlike Xpat RNA, Xpat protein is not exclusively localised to germ plasm. In early oocytes, it is present in nuclei (Figs. 2A, B). In PGCs at stage 28, it was detected within the nuclei (Figs. 2G, H), indeed at later stages Xpat in PGCs appeared principally nuclear (not shown). Xpat was also detected in the nuclei of somatic cells, for example in the ectodermal cells of tailbud embryos, as well as in their cytoplasm (Fig. 2J). Xpat protein was detected in all regions of oocytes and embryos, as confirmed by Western blotting of proteins extracted from dissected oocytes and blastulae (not shown). Although Xpat protein is widespread, the immunofluorescence results indicated that the heaviest concentrations were in the germ plasm and, significantly, only in germ plasm were Xpat particles found clustered together in characteristic aggregates. In the animal

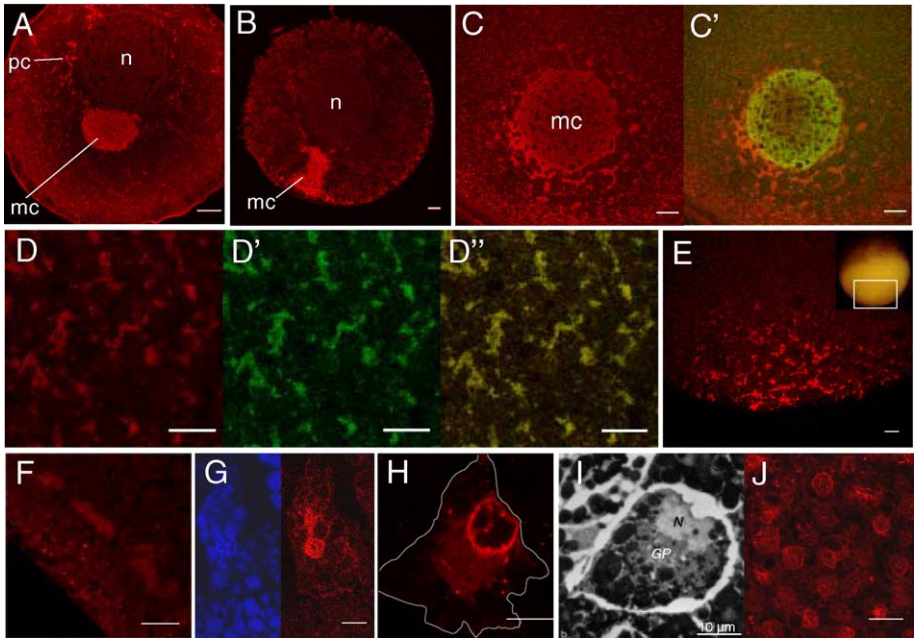

Fig. 2. Xpat protein (red) is a constituent of germ plasm. (A) Anti-Xpat heavily stains particles concentrated in the mitochondrial cloud (mc) of a stage I oocyte, and pre-clouds (pc) around the nucleus (n). (B, C) At stage II, Xpat is still focused in the mitochondrial cloud, along with endogenous Xpat mRNA, detected by injecting fluorescent antisense Xpat (green, overlay, C′). This oocyte is viewed looking in from the point where the mitochondrial cloud touches the cortex. (D) Germ plasm islands in the vegetal cortex of a stage VI oocyte, detected by anti-Xpat (D), mitochondrial anti-VDAC (D′, overlay in D″). (E) Field of germ plasm islands at the vegetal pole (see inset of the unfertilised egg). (F) Islands at the 2-cell stage, shown in transverse optical section. (G) A PGC deep in the endoderm of a stage 28 embryo, also stained with DAPI (left, blue). (H) A PGC, immunostained for Xpat, and the cellular outline drawn in grey, demonstrates similarity to a conventionally stained PGC in the tailbud embryo (I), from Kamimura et al. (1980). (J) Nuclei in epidermal cells of tailbud embryos also contain Xpat. Scale bars, 20 μm.

hemisphere, particles remain isolated. Cytoplasmic Xpat was also detected as particles in somatic cells, but became non-particulate and perinuclear in late-staged PGCs. Nuclear Xpat is generally non-particulate. Therefore, while Xpat is found elsewhere in the cell, it is more concentrated in, and it takes on unique structural qualities in the germ plasm.

Xpat protein can cause the formation and localisation of germ plasm-like structures

With the knowledge that Xpat is a major constituent of germ plasm, we wanted to address its possible functions there. Unfortunately, because of the large maternal source of Xpat protein, loss-of-function experiments, in which mRNA is depleted, would probably be uninformative. We adopted the hypothesis that Xpat might be involved in forming and locating germ plasm and therefore we examined the behaviour of exogenous GFP-tagged Xpat protein in oocytes.

We injected an mRNA encoding an Xpat-GFP fusion protein into full-grown oocytes, targeting the equator region, and cultured them under conditions that are known to support the localisation of RNAs to the vegetal pole by the late pathway (Yisraeli and Melton, 1988). The essential feature of the culture medium is that it includes the yolk protein precursor vitellogenin, which allows oocyte growth by endocytosis and, since this is essential for RNA localisation, it could also permit proteins to localise. It is important to note that the Xpat-GFP RNA lacks Xpat UTRs, and therefore is not itself localised in the oocyte (data not shown), as was previously shown for a LacZ fusion (Hudson and Woodland, 1998). After overnight culture, Xpat-GFP was observed to form small particles, which accumulated in a region surrounding the equatorial injection site of mRNA (Figs. 3B–D). After another 1–2 days of culture, the particles had relocated to the vegetal pole (Figs. 3E, F), while GFP did not form particles and remained uniformly distributed in control injected oocytes (Fig. 3G). We believe that the particles translocated, rather than dissociating and reforming at the vegetal pole, because we were able to observe particles moving at speeds compatible with motor-based transport (see below). At the vegetal pole of stage VI oocytes, the Xpat-GFP particles aggregated into large structures remarkably similar in size, shape and distribution to germ plasm islands (compare Fig. 3E with the distribution of Xpat mRNA in the germ plasm islands in the egg; Fig. 3A), as well as that of the endogenous protein (Fig. 2E). At high magnification, the Xpat-GFP structures could be seen to be aggregates of smaller particles, and to strongly resemble endogenous germ plasm islands revealed by immunostaining of Xpat (Figs. 3I, J). It will also be seen from the bisected oocytes that a non-particulate form of Xpat accumulates in the nucleus. This correlates with the antibody staining results on small oocytes and embryonic cells.

We tested whether the fields of Xpat-GFP structures behaved like endogenous germ plasm islands following hormone-induced oocyte maturation and fertilisation. Oocytes exhibiting vegetal fields of aggregated Xpat particles were treated with progesterone to induce maturation, then prick-activated to simulate fertilisation. The Xpat-GFP fields progressively contracted as the oocyte progressed through maturation and the first cell cycle, in line with the behaviour of endogenous germ plasm islands (Fig. 4). We conclude that the Xpat-GFP aggregates associate with the cortical cytoskeleton in a way that enables them to behave like the endogenous germ plasm islands.

Taken together, the Xpat GFP expression experiments in Stage VI oocytes show that Xpat protein has the ability to translocate to the vegetal cortex in full-grown oocytes and to assemble into structures which look and behave like germ plasm islands. This is intriguing since endogenous germ plasm normally forms and localises to the vegetal cortex much earlier during oogenesis, and it is generally assumed that its formation is restricted to these early stages.

To examine the behaviour of Xpat protein in oocytes during the period when germ plasm formation is active, as indicated by the localisation of specific RNAs such as *Xcat2*, we expressed Xpat-GFP in stage I oocytes. When expressed at high levels, the protein formed particles and accumulated at sites of endogenous Xpat concentration: in the pre-clouds and around and within the mitochondrial cloud itself (Figs. 3K, L). Some Xpat-GFP particles were observed to show rapid translocation in the cytoplasm, with rapid bursts of linear movement (Supplementary video). Of 18 particles that could be clearly tracked by video microscopy, 50% moved towards the mitochondrial cloud (9/18), 22% moved away from it (4/18) and 28% moved perpendicularly to the confocal plane (5/18). Thus, more than twice as many particles moved towards the cloud than away from it. Maximum speeds calculated along linear paths ranged from 0.48 to 0.84 μm/s (average for 19 particles analysed from three image sequences: 0.7 μm/s) and the distances travelled along linear paths within single confocal planes ranged from 2.0 to 8.4 μm (mean 4.6 μm, $n = 18$). These motility properties are very similar to those reported for microtubule motor-based transport in other cell types (Smith and Simmons, 2001). Similar movement of particles was also observed in stage VI oocytes (not shown). These results suggest that Xpat translocates in the oocyte by association with microtubule-based motors, a behaviour which may lead to its accumulation in the MC (see below).

Xpat can organise an ectopic germ-plasm-like field

We next asked whether exogenous Xpat was capable of directing ectopic assembly of structures resembling germ plasm. For this purpose, we created mislocalised fields of Xpat-GFP structures by injecting mRNA into the animal hemisphere of stage VI oocytes and omitting vitellogenin from the medium to impair particle transport. In this way, fields of structures closely resembling endogenous vegetal germ plasm fields could be obtained in the animal hemisphere (Fig. 3H). The endogenous germ plasm, revealed by staining of mitochondria remained at the vegetal pole (not shown). If very high levels of Xpat mRNA were introduced, granules formed over the entire oocyte (not shown). Xpat-GFP could also form granular aggregates in somatic cells of *Xenopus*

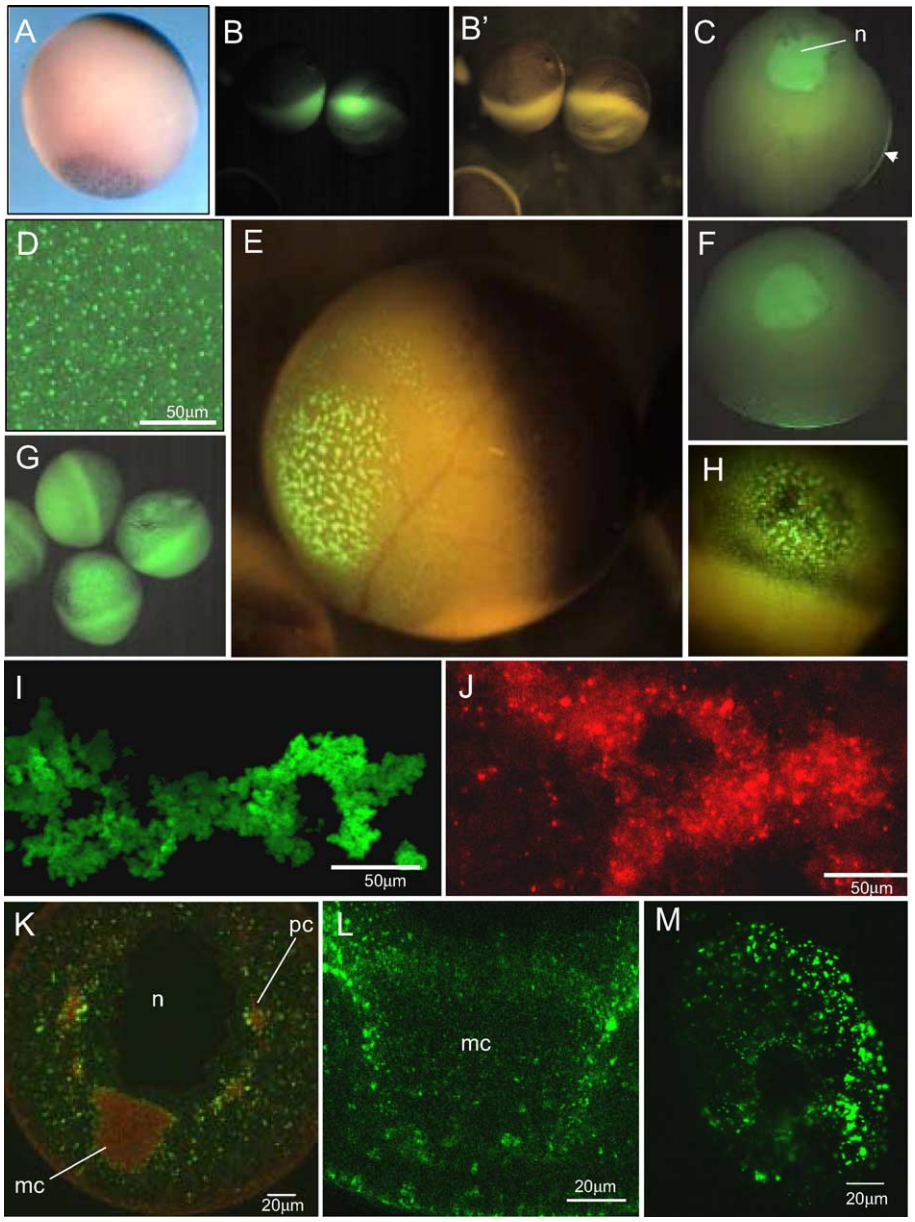

Fig. 3. Exogenously expressed Xpat organises germ plasm-like structures. (A) In situ hybridisation to Xpat mRNA in the unfertilised egg. (B–F) Fluorescence after equatorial injection of Xpat-GFP mRNA. At 18 h, the Xpat-GFP was around the injection point (B, fluorescence, B′, white light) and localised to the cortex (white arrowhead in bisected oocyte, C) as well as the nucleus, n (D). At the cortex, it was particulate. By 55 h, the fluorescent particles moved to the vegetal pole and formed a field of germ plasm-like aggregates (E) in the cortex (F). (G) Control GFP was uniformly distributed in the oocyte. (H) In the absence of vitellogenin, a similar field of Xpat-GFP structures formed in the pigmented animal pole. (I) An Xpat-GFP vegetal aggregate is similar in structure to endogenous Xpat germ islands revealed by anti-Xpat antibody (J). (K, L) In stage I oocytes, 24 h after injection, Xpat-GFP forms particles, accumulating around the mitochondrial cloud (mc) and pre-clouds (pc). (M) Xpat-GFP granules in an epidermal cell of a neurula.

embryos (Fig. 3M). These results show that ectopically expressed Xpat can form germ plasm-like aggregates in the animal pole, or cells derived from it, and suggest that aggregate formation may only require Xpat at critical concentrations to self-assemble ectopically.

To establish if the structures formed from Xpat-GFP contained other germ plasm components, we stained vegetal or ectopic fields of Xpat for mitochondria, either in live oocytes using the vital dye TMRE (tetramethylrhodamine ethyl ester), or in fixed oocytes by anti-VDAC immunofluorescence (Fig. 5). Vegetal Xpat-GFP aggregates were found to be situated slightly more superficially than endogenous germ plasm islands, and appeared to attract the mitochondria of the germ plasm layer into surrounding annuli (Figs. 5A, B, C). In some oocytes in which large Xpat-GFP aggregates formed, mitochondria became completely integrated into the Xpat-GFP islands, not only those situated around the vegetal pole but also those that formed ectopically in the animal hemisphere (Figs. 5D, E). We conclude that Xpat can organise large structures ectopically in stage VI oocytes with at least some characteristics of germ plasm. We would not expect these ectopic structures to have an identical composition to endogenous germ

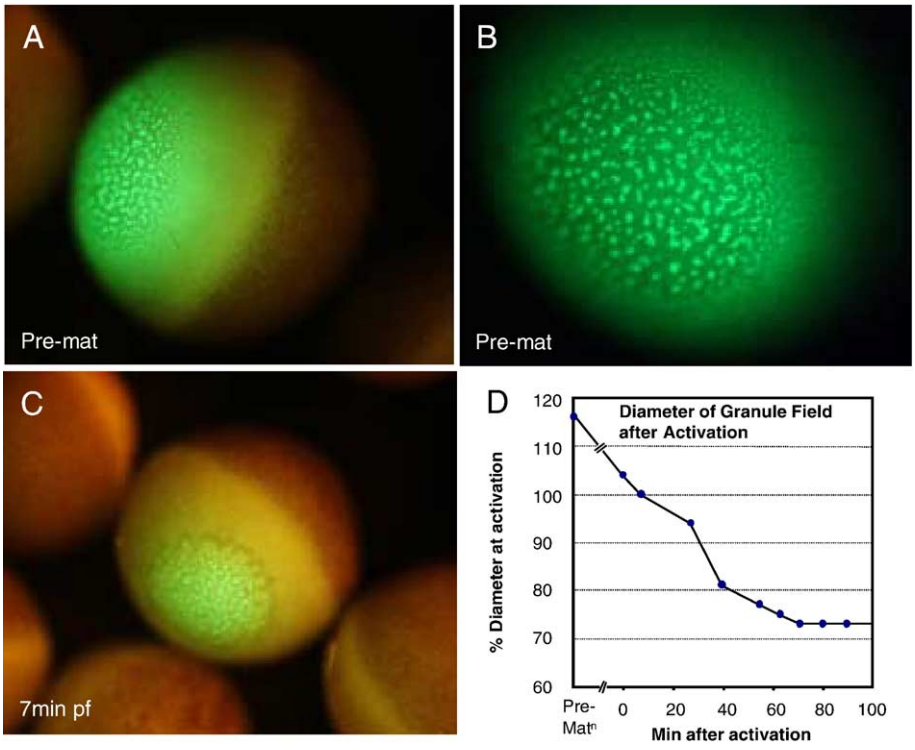

Fig. 4. The vegetal field of Xpat-GFP aggregates contracts during maturation and fertilisation, like endogenous germ plasm. (A) A field of Xpat-GFP aggregates at the vegetal pole of a stage VI oocyte before maturation, seen with a combination of fluorescence and white light, or (B) with fluorescence alone. (C) The same oocyte after maturation, then pricked to simulate fertilisation and left for 7 min. (D) The decrease in size of the field of large granules through maturation, pricking at a time equivalent to the first cell cycle. Maturation took 6 h after progesterone addition and the oocyte was pricked at 6.5 h.

plasm, because many specific germ plasm components, including the localised RNAs, are not available for recruitment at this time. Germ plasm RNAs are localised in the vegetal germ plasm islands at earlier stages and no new transcripts are made in stage VI oocytes (Zhou and King, unpublished observations). We tested if microinjected, fluorescently labelled *Xcat2* mRNA could localise into the Xpat-GFP aggregates at stage VI (data not shown). The mRNA formed small particles throughout the vegetal pole, typical of localisation by the late pathway, as is found without Xpat-GFP expression. This may mean that additional proteins are needed for localisation into the germ plasm, and these are not in excess in the late oocyte. Alternatively, when the late pathway becomes active at the onset of oogenesis, it dominantly diverts mRNAs like *Xcat2* away from the germ plasm, which is possible because the UTR sequences used by both pathways are similar.

Microtubule-mediated transport and assembly of Xpat-GFP particles

The observation of rapid-directed movement of Xpat-GFP particles in oocyte cytoplasm and of linear “tracks” of endogenous and exogenous Xpat particles in stage I oocytes (Fig. 3L) suggested that cytoskeletal-based transport of Xpat particles may participate in germ plasm assembly. We confirmed that Xpat associates with microtubules by fixing normal and Xpat-GFP expressing oocytes and processing them for anti-tubulin immunofluorescence. In stage I oocytes, endogenous Xpat particles were clearly found to align with microtubules (Fig. 6A). In stage VI oocytes, dense microtubules were concentrated in and around the Xpat-rich germ plasm islands (Fig. 6B). Xpat-GFP structures in equatorial regions of stage VI oocytes, away from endogenous germ plasm also became associated with dense foci of microtubules (Fig. 6C).

We used drug treatments to test the involvement of microtubules and microfilaments in the formation of Xpat-GFP particles, their translocation to the vegetal pole and their assembly into larger, germ plasm-like structures in stage VI oocytes. Nocodazole, which disrupts microtubules, had no effect on particle formation around the injection site, but prevented their aggregation and localisation to the vegetal cortex at 48 h, such that after 3 days there was no concentration at the vegetal pole (compare Figs. 6D, E with F, G). These results were replicated using colcemid, which also disrupts microtubules (data not shown). Thus, microtubules are necessary for complete localisation of Xpat-GFP particles to the vegetal pole and for their assembly into larger structures, while particle formation appears not to require microtubules.

Some initial localisation of Xpat-GFP particles to the vegetal pole was observed in the presence of microtubule disrupting drugs. This could be explained by the resistance of a small, stable microtubule sub-population to the inhibitors (Chang et al., 2004; Gard, 1991), as was also found in *C. elegans* (Gotta and Ahringer, 2001; Hird et al., 1996). Treatment with taxol, which stimulates microtubule polymerisation, stabilises existing microtubules and induces their bundling, caused the pigment to assume a honeycomb pattern

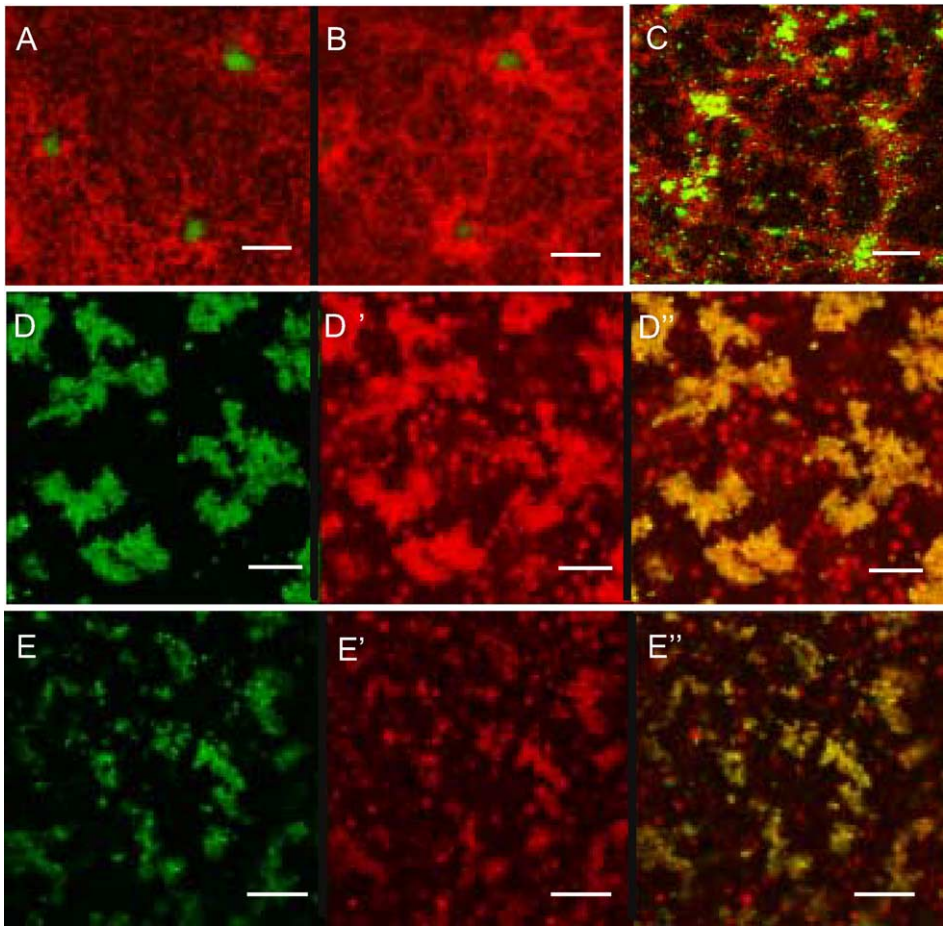

Fig. 5. Xpat-GFP recruits mitochondria. Xpat-GFP is shown in green and mitochondria by staining with TMRE (red) after 2 days incubation. (A, B) Xpat-GFP aggregates in the vegetal hemisphere drew in mitochondria from deeper layers, shown in two optical sections of living oocytes 1.6 μm apart. (C) Anti-VDAC staining (red) of fixed Xpat-GFP-expressing oocytes confirmed this result. (D) In some cases, mitochondria (D′) became integrated into the Xpat-GFP aggregates (D; overlay D″). (E) The same is seen in aggregates formed in the animal hemisphere, after animal mRNA injection and omitting vitellogenin. Scale bars, 20 μm, A–C; 10 μm, D–E.

(not shown). The Xpat-GFP particles became arranged in lines along the clear pathways between the pigment areas in the cortex, suggesting that they associate with stabilised bundles of microtubules induced by taxol, and the localisation to the cortex was less complete (Figs. 6H, I).

A corollary of the proposal that Xpat-GFP particles are transported to the vegetal pole or the mitochondrial cloud via microtubules is that there is a polarised organisation of microtubules in oocytes. In very early *Xenopus* oocytes, microtubule minus ends are likely to be concentrated in the nascent mitochondrial cloud and pre-clouds, as indicated by the distribution of the centrosomal component γ-tubulin and of the microtubule nucleating activity (Gard, 1994; Gard et al., 1995; Kloc and Etkin, 1998). In stage VI oocytes, there are no defined microtubule nucleation sites, but γ-tubulin is found to be most concentrated in small punctae very close to the vegetal surface, as well as around the nucleus (Gard, 1994). This indicates that microtubule minus ends are present at the cortex, as demonstrated by Pfeiffer and Gard (1999), and that there is an overall polarisation towards the vegetal pole. We thus addressed the possibility that the microtubule-dependent transport of Xpat-GFP to the vegetal cortex of stage VI oocytes involves the minus end-directed motor cytoplasmic dynein, and examined whether dynein is associated with germ plasm islands and Xpat-GFP particles by immunofluorescence.

In the vegetal cortical region of stage VI oocytes, dynein was detected in scattered foci, as well as in the germ plasm islands, where it largely co-localised with Xpat protein (Figs. 6L–L″). Particles of expressed Xpat-GFP also stained intensely with anti-dynein antibodies, the dynein appearing to coat the GFP particles (Figs. 6M–M″). The heavy anti-dynein IC staining of the Xpat-GFP structures compared with endogenous germ plasm may reflect a ready interaction of freshly introduced Xpat protein with the microtubule transport system, while Xpat in the germ plasm island has long completed the localisation process. Consistent with this, we have found that mature germ plasm islands are not disrupted by microtubule depolymerising agents (unpublished observations). These observations fit the hypothesis that Xpat is transported via dynein to microtubule minus ends, explaining the relocation of Xpat-GFP particles to the vegetal cortex of stage VI oocytes, and their rapid linear movement in stage I oocytes.

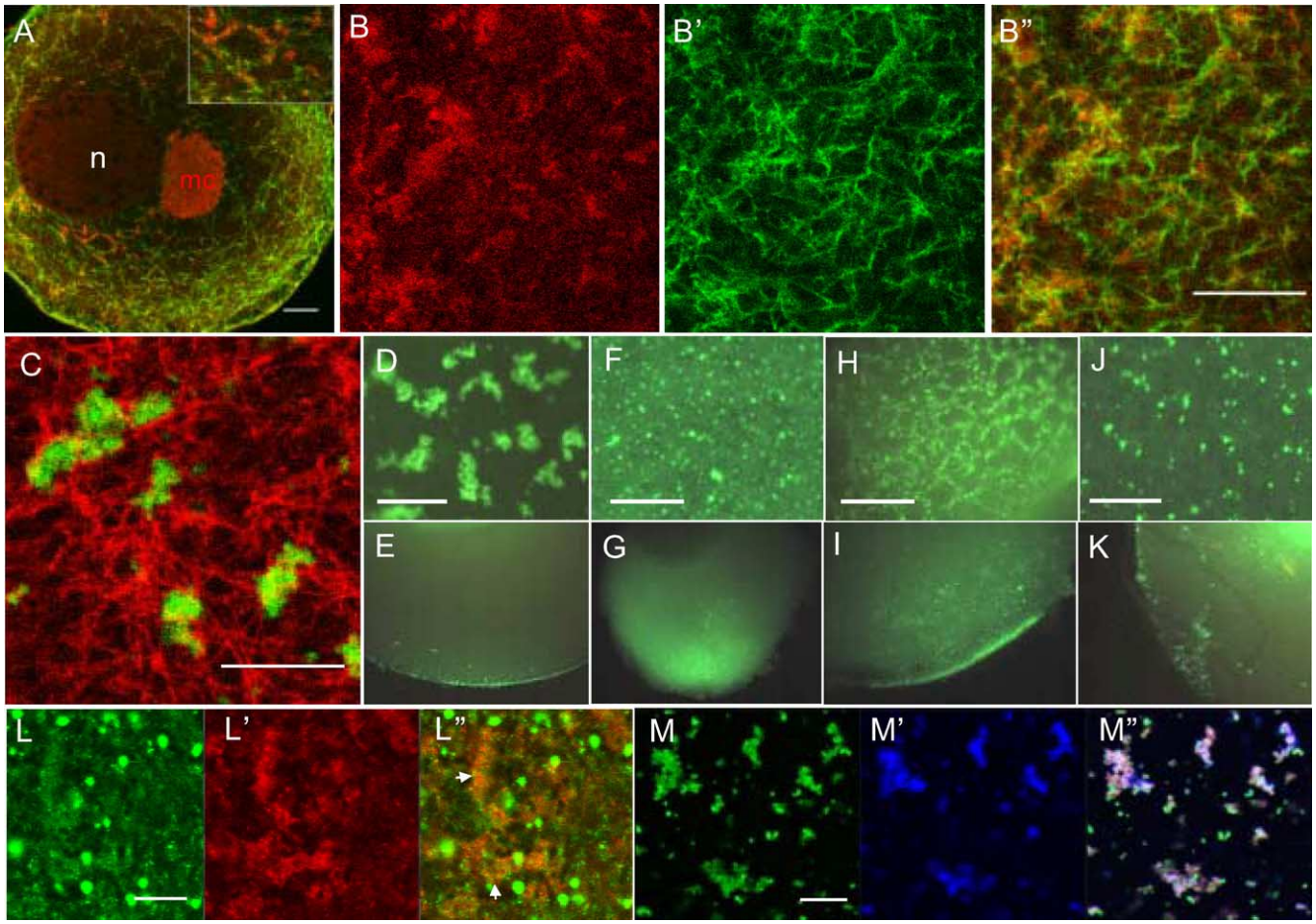

Fig. 6. Microtubule-based transport of Xpat. (A) In stage I oocytes, Xpat particles (Anti-Xpat, red) are closely associated with microtubules (green), here shown by immunofluorescence. (B–B′ and B″) Xpat germ plasm islands in stage VI oocytes (red) are in dense areas of microtubules (green, overlay B′ and B″), as are Xpat-GFP aggregates (C, Xpat-GFP green, microtubules in red). (D–K) Effects of inhibitors on Xpat-GFP. In control oocytes, Xpat-GFP forms cortical particles at the equator by 18 h after mRNA injection (see Fig. 3D). (D, E) These Xpat-GFP particles have formed aggregates at the vegetal cortex by 55 h. (F, G) Nocodazole interferes with vegetal localisation and aggregation, particularly to the cortex. (H, I) Taxol, which bundles microtubules, produces chains of particles all through the oocyte, largely in the cortex. (J, K) Microfilament disruption with cytochalasin D allows some cortical localisation, but the cortex appears to fragment and the particles form only small, disorganised aggregates, largely at the vegetal pole. (L–L″) Dynein, stained with an intermediate chain antibody (green) is present in intense local foci in the cortex and also as fine particles in germ plasm islands (arrows), identified with Xpat antibody (red). (L″) Overlay. (M–M″) Xpat-GFP (green) co-localises with immunostained Dynein (blue). Overlay (M″). 20 μm scale bars in confocal sections (A–C), 4 μm (L), 10 μm (M). 50 μm scale bars in surface views of oocytes (D–J). Panels E, G, I and K are bisected oocytes, fixed at 80°C for 30 s; the control section is Fig. 3F.

Microfilaments are needed for the aggregation of Xpat-GFP particles

As with microtubule disruption, destabilising the microfilament network prevented the assembly of large island-like structures from Xpat-GFP particles. Cytochalasin D resulted in the appearance of small disorganised cortical aggregates, most likely reflecting disruption of the cortical cytokeratin network following microfilament disruption (Figs. 6J, K) (Gard et al., 1997), an effect previously described for Vg1 mRNA localisation (Alarcon and Elinson, 2001). In addition, the tight cortical location of the Xpat-GFP particles was lost (Fig. 6K), another symptom of the general disruption of cortical organisation. Cytochalasin treatment did not affect the formation of the small Xpat-GFP particles, nor their translocation to the vegetal pole.

To summarise the data concerning the relationship of Xpat with the cytoskeleton, we find that neither microtubules nor microfilaments are required for small Xpat particles to form, but that their transport to the vegetal region occurs via microtubules, most likely by a mechanism involving minus-end-directed transport. Assembly of Xpat particles into germ-plasm-like islands in the actin-rich cortical region and Xpat cortical localisation require both filament systems.

Discussion

Our results show that Xpat protein, like *Xpat* RNA, is a major constituent of *Xenopus* germ plasm and suggest that it plays a role in its localisation, formation and maintenance. Traditionally, germ plasm formation has been thought to occur by a series of successive, discrete steps during the months taken to complete oogenesis: the formation of the mitochondrial cloud with its associated RNAs, its bulk movement to the developing vegetal pole cortex and finally its fragmentation into individual islands (Houston and King, 2000b; Kloc et al., 2001). Our finding that Xpat protein can be transported to the

vegetal pole and forms germ-plasm-like structures, even in fully grown oocytes, suggests that germ plasm formation and/or the maintenance of its structure may rather be an active, ongoing process. In this respect, the circularity of the fields, both vegetal and ectopic, and their tight cortical localisation are notable. These features are not simply a consequence of the positioning of the injected Xpat mRNA, since injected mRNAs lacked the sequences required for mitochondrial cloud localisation and became irregularly distributed in the oocyte (not shown). The cortical location and aggregation indicate that the ectopic Xpat protein interacts with the cytoskeleton in such a way as to govern its own distribution. Of course, in normal oogenesis, the localisation of *Xpat* mRNA to the germ plasm may also contribute to the localisation of the protein. Alternatively, the Xpat mRNA molecules that are translated in oocytes might not actually be those that are localised to germ plasm, indeed other RNAs incorporated into germ plasm have been found to be translationally inactive (Houston and King, 2000a; MacArthur et al., 1999; Mosquera et al., 1993).

The precise role of Xpat in the germ plasm remains to be established. Unfortunately, we could not test the effects of loss of Xpat function by antisense oligonucleotide-mediated depletion of mRNA because of the large amount of maternal protein. Also, if the function of Xpat is in organising germ plasm components, cleavage and development in *Xenopus* are so rapid that ectopic expression in the embryo would not permit introduced Xpat-GFP to perform this function (which normally takes weeks or months) before it is compartmentalised into blastula cells. Indeed our study strongly suggests that Xpat functions to gather germ plasm components, including mitochondria, at microtubule minus ends, an activity that could both drive the initial formation of the mitochondrial cloud and maintain the integrity and position of germ plasm islands throughout later oogenesis. In oocytes, Xpat-GFP appeared to organise local foci of microtubules. Such an activity may contribute to the gathering of particles into germ plasm-like aggregates and the incorporation of other components like mitochondria. Xpat particle aggregation also requires microfilaments, which are concentrated in the cortical region where the germ plasm-like aggregates are found. During later stages of embryogenesis, interactions between Xpat protein and microtubule minus ends could be involved in the processes that concentrate germ plasm into five or so PGCs in the blastula.

While we have shown that Xpat forms structures that look like germ plasm and, like germ plasm, contain mitochondria, our ability to test for assembly of other components is limited by our knowledge of germ plasm composition, particularly concerning proteins. We tested whether exogenous *Xcat2* RNA could be assembled into the Xpat-GFP particles but found no evidence to support co-assembly (not shown). This is true even of exogenously supplied mRNA. In large oocytes, this is not surprising because the late RNA localisation pathway becomes dominant after stage II such that germ plasm RNAs injected into late stage oocytes localise to the vegetal cortex, but do not associate with germ plasm (Zhou and King, 1996b). Components that function to localise these RNAs correctly may well be unavailable in later stage oocytes, because they are either absent or sequestered within the germ plasm. Alternatively, when they are present, the late pathway proteins may override the effects of those of the early pathway.

The significance of the Xpat particles detected outside the germ plasm by immunofluorescence and the importance of the nuclear Xpat remain to be understood. Since ectopic Xpat-GFP appears to be able to initiate germ plasm formation in the animal hemisphere, it is somewhat surprising that endogenous Xpat protein in the animal half of the oocyte does not do so. Explanations may be deduced from the observations that overexpressed Xpat-GFP shows a much more complete localisation to the vegetal pole than endogenous Xpat, while injection of even larger amounts of Xpat-GFP mRNA leads to aggregates forming all over the oocyte cortex. Therefore, one possibility is that the endogenous particles in the animal hemisphere represent a pool of protein not competent to associate with microtubules, and thus unable to translocate to the vegetal pole or to initiate germ plasm formation. More likely, the concentration of Xpat particles in this region may be maintained below the threshold for aggregate formation by their ongoing active transport towards the vegetal pole. Sites in the animal pole where Xpat may be sequestered from the transport machinery may be limited and saturated, so that additional Xpat is transported away. A comparable, and possibly related asymmetry is shown by γ-tubulin, which is present all over the cortex, but concentrated at the vegetal pole (Gard, 1994). As embryonic development proceeds, it appears that specific changes occur in the PGCs which alter Xpat behaviour. The cytoplasmic somatic Xpat in tailbud embryos remains particulate, while that in the PGCs is non-particulate and has coalesced into a perinuclear mass, the nuage structure. It will be of interest to uncover the factors that regulate this change in behaviour.

The fact that a fraction of both endogenous and exogenous Xpat is nuclear suggests that Xpat might have a role in the nucleus. Examination of the protein sequence showed a putative nuclear location sequence (NLS) towards the C-terminus, indeed when the C-terminus is deleted, nuclear enrichment is lost. This sequence (underlined) KRFVLG-**PKEKRKIK** is related to the bipartite NLS of Nucleoplasmin, KRPAATKKAGQAKKKK although the spacing is different. There is also similarity to the NLS of SV40 (bold), **PKKKRK**. In a preliminary mutagenic analysis (unpublished data), we showed that the initial KR residues were essential for nuclear location in oocytes and HeLa cells, but the terminal KXR was not. In addition, the intact bipartite sequence was not sufficient to direct nuclear location of GFP. Thus, there seems to be an NLS with some novel features.

The function of germ plasm as a germ line determinant is similar in diverse animals, yet the molecules involved are largely different. Despite their different identities, germ plasm proteins show some equivalent properties. In *C. elegans*, PIE-1 is a unique germ granule component which, like Xpat, shows nuclear and, from our unpublished data on cultured cells, centrosomal localisation (Cuenca et al., 2003; Mello et al., 1996). Xpat also shows certain parallels with Oskar in

Drosophila. Both are present in germ plasm as RNA and protein and in the adult are restricted to the female germ line (unpublished data for Xpat). Both are capable of making ectopic germ plasm-like particles. In *Drosophila*, however, this process depends on the localisation of the mRNA alone; the protein forms germ granules wherever it is synthesised. In contrast, both Xpat RNA (Hudson and Woodland, 1998) and protein produced from non-localised RNAs are capable of localisation. In *Drosophila*, the ectopic germ granules have been shown to be fully functional in directing germ line development (Ephrussi and Lehmann, 1992; Smith et al., 1992). This kind of experiment, relying on ectopically expressing Oskar throughout oogenesis and utilising bicoid mRNA control sequences, is not currently possible in *Xenopus*, because, while transgenesis with mutated Xpat genes could be achieved, mutations which would mislocalise the protein, rather than the RNA, have yet to be discovered.

It is remarkable how frequently germ plasm proteins are novel and show tight phylogenetic restriction; for example, Oskar is restricted to dipteran flies and PIE-1 to nematodes. In *Xenopus*, Xpat and Germes are proteins for which homologues have not yet been identified outside the genus *Xenopus* [there has been a report that in in situ hybridisation, an Xpat probe cross hybridises with an mRNA in cricket oocytes (Bradley et al., 2001), but this needs sequence authentication]. This raises interesting evolutionary questions as to how and why such a fundamental process as germ line formation can be subject to non-conserved, presumably rapidly evolving mechanisms.

Acknowledgments

This work was started by Dr Clare Hudson, who provided the in situ in Fig. 3A and offered critical comments on the manuscript. We thank Christian Rouvière for particle movement analysis and Dr. M. Colombini for anti-VDAC serum. The company of Biologists granted permission to reprint Fig. 2I. We thank the Wellcome Trust, MRC, BBSRC, CNRS, ARC and NIH (GM-33932) (MLK) for support.

Appendix A. Supplementary data

Supplementary data associated with this article can be found, in the online version, at doi:10.1016/j.ydbio.2005.08.044.

References

Alarcon, V.B., Elinson, R.P., 2001. RNA anchoring in the vegetal cortex of the *Xenopus* oocyte. J. Cell Sci. 114, 1731–1741.

al-Mukhtar, K.A., Webb, A.C., 1971. An ultrastructural study of primordial germ cells, oogonia and early oocytes in *Xenopus laevis*. J. Embryol. Exp. Morphol. 26, 195–217.

Beckhelling, C., Chang, P., Chevalier, S., Ford, C., Houliston, E., 2003. Pre-M phase-promoting factor associates with annulate lamellae in *Xenopus* oocytes and egg extracts. Mol. Biol. Cell 14, 1125–1137.

Berekelya, L.A., Ponomarev, M.B., Luchinskaya, N.N., Belyavsky, A.V., 2003. *Xenopus* Germes encodes a novel germ plasm-associated transcript. Gene Expr. Patterns 3, 521–524.

Betley, J.N., Frith, M.C., Graber, J.H., Choo, S., Deshler, J.O., 2002. A ubiquitous and conserved signal for RNA localization in chordates. Curr. Biol. 12, 1756–1761.

Bilinski, S.M., Jaglarz, M.K., Szymanska, B., Etkin, L.D., Kloc, M., 2004. Sm proteins, the constituents of the spliceosome, are components of nuage and mitochondrial cement in *Xenopus* oocytes. Exp. Cell Res. 299, 171–178.

Bradley, J.T., Kloc, M., Wolfe, K.G., Estridge, B.H., Bilinski, S.M., 2001. Balbiani bodies in cricket oocytes: development, ultrastructure, and presence of localized RNAs. Differentiation 67, 117–127.

Bubunenko, M., Kress, T.L., Vempati, U.D., Mowry, K.L., King, M.L., 2002. A consensus RNA signal that directs germ layer determinants to the vegetal cortex of *Xenopus* oocytes. Dev. Biol. 248, 82–92.

Chang, P., Torres, J., Lewis, R.A., Mowry, K.L., Houliston, E., King, M.L., 2004. Localization of RNAs to the mitochondrial cloud in *Xenopus* oocytes through entrapment and association with endoplasmic reticulum. Mol. Biol. Cell 15, 4669–4681.

Choo, S., Heinrich, B., Betley, J.N., Chen, Z., Deshler, J.O., 2005. Evidence for common machinery utilized by the early and late RNA localization pathways in *Xenopus* oocytes. Dev. Biol. 278, 103–117.

Claussen, M., Horvay, K., Pieler, T., 2004. Evidence for overlapping, but not identical, protein machineries operating in vegetal RNA localization along early and late pathways in *Xenopus* oocytes. Development 131, 4263–4273.

Clements, D., Friday, R.V., Woodland, H.R., 1999. Mode of action of VegT in mesoderm and endoderm formation. Development 126, 4903–4911.

Cook, J.P., Savage, P.M., Lord, J.M., Roberts, L.M., 1993. Biologically-active interleukin 2-ricin A-chain fusion proteins may require intracellular proteolytic cleavage to exhibit a cytotoxic effect. Bioconjugate Chem. 4, 440–447.

Cuenca, A.A., Schetter, A., Aceto, D., Kemphues, K., Seydoux, G., 2003. Polarization of the *C. elegans* zygote proceeds via distinct establishment and maintenance phases. Development 130, 1255–1265.

Czolowska, R., 1972. The fine structure of "germinal cytoplasm" in the egg of *Xenopus laevis*. Wilhelm Roux's Arch. Entwicklungsmech. Org. 169, 335–344.

Ephrussi, A., Lehmann, R., 1992. Induction of germ cell formation by Oskar. Nature 358, 387–392.

Extavour, C.G., Akam, M., 2003. Mechanisms of germ cell specification across the metazoans: epigenesis and preformation. Development 130, 5869–5884.

Fukui, A., Komazaki, S., Miyoshi, O., Asashima, M., 2003. Immunocytochemical study of activin type IB receptor (XALK4) in *Xenopus* oocytes. Dev. Growth Differ. 45, 113–119.

Gard, D.L., 1991. Organization, nucleation, and acetylation of microtubules in *Xenopus laevis* oocytes: a study by confocal immunofluorescence microscopy. Dev. Biol. 143, 346–362.

Gard, D.L., 1994. Gamma-tubulin is asymmetrically distributed in the cortex of *Xenopus* oocytes. Dev. Biol. 161, 131–140.

Gard, D.L., Affleck, D., Error, B.M., 1995. Microtubule organization, acetylation, and nucleation in *Xenopus laevis* oocytes: II. A developmental transition in microtubule organization during early diplotene. Dev. Biol. 168, 189–201.

Gard, D.L., Cha, B.J., King, E., 1997. The organization and animal-vegetal asymmetry of cytokeratin filaments in stage VI *Xenopus* oocytes is dependent upon F-actin and microtubules. Dev. Biol. 184, 95–114.

Gotta, M., Ahringer, J., 2001. Axis determination in *C. elegans*: initiating and transducing polarity. Curr. Opin. Genet. Dev. 11, 367–373.

Heasman, J., Quarmby, J., Wylie, C.C., 1984. The mitochondrial cloud of *Xenopus* oocytes—The source of germinal granule material. Dev. Biol. 105, 458–469.

Hird, S.N., Paulsen, J.E., Strome, S., 1996. Segregation of germ granules in living *Caenorhabditis elegans* embryos: cell-type-specific mechanisms for cytoplasmic localisation. Development 122, 1303–1312.

Houston, D.W., King, M.L., 2000a. A critical role for Xdazl, a germ plasm-localized RNA, in the differentiation of primordial germ cells in *Xenopus*. Development 127, 447–456.

Houston, D.W., King, M.L., 2000b. Germ plasm and molecular determinants of germ cell fate. Curr. Top. Dev. Biol. 50, 155–181.

Hudson, C., Woodland, H.R., 1998. Xpat, a gene expressed specifically in germ plasm and primordial germ cells of *Xenopus laevis*. Mech. Dev. 73, 159–168.

Ikenishi, K., Tanaka, T.S., Komiya, T., 1996. Spatiotemporal distribution of the protein of *Xenopus*-Vasa homolog (*Xenopus*-Vasa-Like Gene 1, Xvlg1) in embryos. Dev. Growth Differ. 38, 527–535.

Kamimura, M., Kotani, M., Yamagata, K., 1980. The migration of presumptive primordial germ cells through the endodermal cell mass in *Xenopus laevis*: a light and electron microscopic study. J. Embryol. Exp. Morphol. 59, 1–17.

King, M.L., Zhou, Y., Bubunenko, M., 1999. Polarizing genetic information in the egg: RNA localization in the frog oocyte. BioEssays 21, 546–557.

King, M.L., Messitt, T.J., Mowry, K.L., 2005. Putting RNAs in the right place at the right time: RNA localization in the frog oocyte. Biol. Cell 97, 19–33.

Kloc, M., Etkin, L.D., 1995. Two distinct pathways for the localization of RNAs at the vegetal cortex in *Xenopus* oocytes. Development 121, 287–297.

Kloc, M., Etkin, L.D., 1998. Apparent continuity between the messenger transport organizer and late RNA localization pathways during oogenesis in *Xenopus*. Mech. Dev. 73, 95–106.

Kloc, M., Etkin, L.D., 1999. Analysis of localised RNAs in *Xenopus* oocytes. In: Richter, J.D. (Ed.), A Comparative Approach to the Study of Oocytes and Embryos. Oxford Univ. Press, New York, pp. 256–267.

Kloc, M., Larabell, C., Etkin, L.D., 1996. Elaboration of the messenger transport organizer pathway for localization of RNA to the vegetal cortex of *Xenopus* oocytes. Dev. Biol. 180, 119–130.

Kloc, M., Larabell, C., Chan, A.P.Y., Etkin, L.D., 1998. Contribution of METRO pathway localized molecules to the organization of the germ cell lineage. Mech. Dev. 75, 81–93.

Kloc, M., Bilinski, S., Chan, A.P.Y., Etkin, L.D., 2000. The targeting of Xcat2 mRNA to the germinal granules depends on a *cis*-acting germinal granule localization element within the 3′ UTR. Dev. Biol. 217, 221–229.

Kloc, M., Bilinski, S., Chan, A.P., Allen, L.H., Zearfoss, N.R., Etkin, L.D., 2001. RNA localization and germ cell determination in *Xenopus*. Int. Rev. Cytol., Surv. Cell Biol. 203, 63–91.

Kloc, M., Dougherty, M.T., Bilinski, S., Chan, A.P., Brey, E., King, M.L., Patrick, C.W., Etkin, L.D., 2002. Three-dimensional ultrastructural analysis of RNA distribution within germinal granules of *Xenopus*. Dev. Biol. 241, 79–93.

Kloc, M., Bilinski, S., Dougherty, M.T., Brey, E.M., Etkin, L.D., 2004. Formation, architecture and polarity of female germline cyst in *Xenopus*. Dev. Biol. 266, 43–61.

Kress, T.L., Yoon, Y.J., Mowry, K.L., 2004. Nuclear RNP complex assembly initiates cytoplasmic RNA localization. J. Cell Biol. 165, 203–211.

Kwon, S., Abramson, T., Munro, T.P., John, C.M., Kohrmann, M., Schnapp, B.J., 2002. UUCAC- and Vera-dependent localization of VegT RNA in *Xenopus* oocytes. Curr. Biol. 12, 558–564.

Lewis, R.A., Kress, T.L., Cote, C.A., Gautreau, D., Rokop, M.E., Mowry, K.L., 2004. Conserved and clustered RNA recognition sequences are a critical feature of signals directing RNA localization in *Xenopus* oocytes. Mech. Dev. 121, 101–109.

MacArthur, H., Bubunenko, M., Houston, D.W., King, M.L., 1999. Xcat2 RNA is a translationally sequestered germ plasm component in *Xenopus*. Mech. Dev. 84, 75–88.

MacArthur, H., Houston, D.W., Bubunenko, M., Mosquera, L., King, M.L., 2000. DEADSouth is a germ plasm specific DEAD-box RNA helicase in *Xenopus* related to eIF4A. Mech. Dev. 95, 291–295.

Mello, C.C., Schubert, C., Draper, B., Zhang, W., Lobel, R., Priess, J.R., 1996. The Pie-1 protein and germline specification in *C. elegans* embryos. Nature 382, 710–712.

Mosquera, L., Forristall, C., Zhou, Y., King, M.L., 1993. A messenger-RNA localized to the vegetal cortex of *Xenopus* oocytes encodes a protein with a Nanos-like zinc finger domain. Development 117, 377–386.

Pfeiffer, D.C., Gard, D.L., 1999. Microtubules in *Xenopus* oocytes are oriented with their minus-ends towards the cortex. Cell Motil. Cytoskeleton 44, 34–43.

Quaas, J., Wylie, C., 2002. Surface contraction waves (SCWs) in the *Xenopus* egg are required for the localization of the germ plasm and are dependent upon maternal stores of the kinesin-like protein Xklp1. Dev. Biol. 243, 272–280.

Santos, A.C., Lehmann, R., 2004. Germ cell formation and migration in *Drosophila* and beyond. Curr. Biol. 14, R578–R589.

Savage, R.M., Danilchik, M.V., 1993. Dynamics of germ plasm localization and its inhibition by ultraviolet irradiation in early cleavage *Xenopus* embryos. Dev. Biol. 157, 371–382.

Smith, D.A., Simmons, R.M., 2001. Models of motor-assisted transport of intracellular particles. Biophys. J. 80, 45–68.

Smith, L.D., Williams, M.A., 1975. Germinal cytoplasm and determination of the primordial germ cells. In: Markert, C.L., Papaconstantinou, J. (Eds.), The Developmental Biology of Reproduction. Academic Press, New York, pp. 3–24.

Smith, J.L., Wilson, J.E., Macdonald, P.M., 1992. Overexpression of Oskar directs ectopic activation of Nanos and presumptive pole cell formation in *Drosophila* embryos. Cell 70, 849–859.

Torpey, N.P., Heasman, J., Wylie, C.C., 1992. Distinct distribution of vimentin and cytokeratin in *Xenopus* oocytes and early embryos. J. Cell Sci. 101, 151–160.

Volodina, N., Denegre, J.M., Mowry, K.L., 2003. Apparent mitochondrial asymmetry in *Xenopus* eggs. Dev. Dyn. 226, 654–662.

Weidinger, G., Stebler, J., Slanchev, K., Dumstrei, K., Wise, C., Lovell-Badge, R., Thisse, C., Thisse, B., Raz, E., 2003. Dead end, a novel vertebrate germ plasm component, is required for zebrafish primordial germ cell migration and survival. Curr. Biol. 13, 1429–1434.

Whitington, P.M., Dixon, K.E., 1975. Quantitative studies of germ plasm and germ cells during early embryogenesis of *Xenopus laevis*. J. Embryol. Exp. Morphol. 33, 57–74.

Wilk, K., Bilinski, S., Dougherty, M.T., Kloc, M., 2005. Delivery of germinal granules and localized RNAs via the messenger transport organizer pathway to the vegetal cortex of *Xenopus* oocytes occurs through directional expansion of the mitochondrial cloud. Int. J. Dev. Biol. 49, 17–21.

Williamson, A., Lehmann, R., 1996. Germ cell development in *Drosophila*. Annu. Rev. Cell Dev. Biol. 12, 365–391.

Wylie, C., 1999. Germ cells. Cell 96, 165–174.

Yisraeli, J.K., Melton, D.A., 1988. The maternal messenger RNA Vg1 is correctly localized following injection into *Xenopus* oocytes. Nature 336, 592–595.

Zearfoss, N.R., Chan, A.P., Wu, C.F., Kloc, M., Etkin, L.D., 2004. Hermes is a localized factor regulating cleavage of vegetal blastomeres in *Xenopus laevis*. Dev. Biol. 267, 60–71.

Zhou, Y., King, M.L., 1996a. Localization of Xcat-2 RNA, a putative germ plasm component, to the mitochondrial cloud in *Xenopus* stage I oocytes. Development 122, 2947–2953.

Zhou, Y., King, M.L., 1996b. RNA transport to the vegetal cortex of *Xenopus* oocytes. Dev. Biol. 179, 173–183.